High Harmonic Generation and the Role of Atomic Orbital Wave Functions

J. Levesque,[1,2] D. Zeidler,[1,3] J. P. Marangos,[4] P. B. Corkum,[1] and D. M. Villeneuve[1,*]

[1]National Research Council of Canada, 100 Sussex Drive, Ottawa, Ontario K1A 0R6, Canada
[2]INRS-Énergie et Matériaux, 1650 boul. Lionel-Boulet, C.P. 1020, Varennes (Québec) J3X 1S2 Canada
[3]Carl Zeiss SMT AG, Rudolf-Eber-Str. 2, 73447 Oberkochen, Germany
[4]The Blackett Laboratory, Imperial College London, Prince Consort Road, London SW7 2BW, United Kingdom

(Received 17 July 2006; published 3 May 2007)

High harmonic spectra were recorded from different rare-gas atoms under identical experimental conditions. It is shown that although each atom's spectrum is different, the differences are due almost entirely to the orbital influence in the recombination step. The amplitude of the continuum electron wave packet versus kinetic energy is derived from these data and is shown to be largely independent of the atom, in agreement with models of tunnel ionization. We compare the measurements with calculations in both the length gauge and the velocity gauge and show that the two gauges imply a different de Broglie wavelength.

DOI: 10.1103/PhysRevLett.98.183903 PACS numbers: 42.65.Ky, 32.80.Wr, 42.65.Re

High harmonic generation (HHG) is a process involving intense femtosecond laser light and gas-phase atoms or molecules [1–3]. It produces a coherent [4], collimated beam of extreme ultraviolet (xuv) radiation that is composed of a train of attosecond pulses. Single attosecond pulses can be isolated and used to probe attosecond time scale motion in atoms, e.g., Auger decay [5]. The radiation has been extended beyond 1 keV in photon energy [6].

High harmonic generation is commonly described using a simple semiclassical explanation involving three steps [7]: (1) tunnel ionization of the highest energy electron, (2) acceleration of the free electron in the laser field, and driving the electron back to the parent ion, and (3) recombination of the electron to the state from which it originated. The recombination step leads to emission of an xuv photon whose energy is given by the sum of the electron's kinetic energy plus the ionization potential of the state. The strong field approximation (SFA) [8] is widely used to model this process semiclassically.

We will show that, for the atoms tested, the first two steps are largely independent of the details of the atom up to an overall scaling constant, and that only the recombination step is sensitive to the particular atom. We will characterize the spectral amplitude of the electronic wave packet that represents the recolliding electron. By combining this amplitude information with phase information [9,10], one can fully reconstruct the recollision electron wave packet.

In addition to characterizing the electron wave packet, this Letter also verifies the model that underlies molecular orbital tomography [11], a method that can measure the three-dimensional shape of a single molecular orbital wave function. A reference atom is used to calibrate the recollision electron wave packet amplitude because an atom has no angular dependence, unlike molecules. We will show that the difference in the HHG spectrum from three different atoms is entirely determined by the shape of the highest occupied orbital, assuming that HHG phase mismatch is negligible.

The experiment has been described previously [11,12]. Briefly, a 30 fs, 800 nm laser pulse from a 50 Hz Ti:Sa laser system was focused into a pulsed gas jet in a vacuum chamber using a 50 cm focal length lens. The thin gas jet was placed in the diverging part of the focus so that short trajectories were phase matched [13]. The resulting xuv radiation was imaged by an xuv spectrometer, and the spectra were recorded on a computer.

In many experiments, efforts are made to maximize the HHG process. On the other hand, in our experiment, every effort was made to ensure that the xuv spectra were a measure of the single-atom response and that propagation effects on the spectra were minimized. Rather than using a gas cell or capillary for the sample gas, a supersonic pulsed valve introduced the gas into the vacuum chamber. The laser beam was focused as close to the 100 μm nozzle as possible, about 1 mm below. With a backing pressure of 3 bars, the gas pressure at this position was estimated to be 14 mbar, and its length was about 1 mm with a Gaussian density profile.

Phase mismatch between the 800 nm driving field and the generated xuv field can lead to an undesired modification of the spectrum. For a gas jet, phase mismatch is mostly due to the differing phase velocities at the two wavelengths, due to the index of refraction of the gas and due to free electrons produced by the intense laser [14,15]. To estimate an upper limit for phase mismatch, we assume a fully ionized gas sample with electron density $n_e = 4 \times 10^{17}$ cm^{-3}. The phase mismatch due to the index of refraction of the gas is negligible compared to the plasma dispersion. The coherence length [15] $L_{\mathrm{coh}} = \pi/\Delta k = 52$ mm, which is much longer than the 1 mm length of the gas jet, so phase mismatch should be minimal in the experiment.

Reabsorption of the xuv radiation could also modify the xuv spectra. Using the total photoionization cross sections

[16], the absorption length [15] $L_{\text{abs}} = 1/(\sigma\rho)$ is greater than 1 mm for He and Ne, and only less than 1 mm for Ar below harmonic 20. We conclude that reabsorption can possibly modify the lowest harmonics of the Ar spectrum. Finally, because we focus well before the gas jet, there is no Gouy phase shift in the medium. These estimates were verified using a two-dimensional HHG propagation code [17] for the case of Ne.

Three different rare gas atoms were chosen to cover a range of ionization potentials and orbital shapes: argon (15.8 eV, $3p$), neon (21.6 eV, $2p$), and helium (24.6 eV, $1s$). While we have only tried three atoms, the different sizes and symmetries of the orbitals enable us to test our hypothesis.

HHG spectra were recorded for each gas sample for a range of laser energies. In Fig. 1, we show the harmonic spectra observed from the three sample atoms. All spectra were recorded under identical laser parameters, with an intensity of 6×10^{14} W/cm^2. Clearly each spectrum has a unique shape. We will show that the shape is determined almost entirely by the shape of the HOMO.

The high harmonic signal can be shown to be related to the transition dipole matrix element between the ground state wave function and a continuum plane wave, as follows [11]. The harmonic emission, in the single-atom model, is proportional to the square of the Fourier transform of the dipole acceleration [18], $\ddot{d}(t)$,

$$S(\Omega) = \left| \int e^{i\Omega t} \ddot{d}(t) dt \right|^2 = \Omega^4 \left| \int e^{i\Omega t} d(t) dt \right|^2. \quad (1)$$

The induced dipole is a measure of the charge displacement within the atom due to the electronic response to the applied field,

$$\mathbf{d}(t) = \langle \psi(\mathbf{r}, t) | \mathbf{r} | \psi(\mathbf{r}, t) \rangle. \quad (2)$$

If we separate the electronic wave function $\psi(\mathbf{r}, t)$ into two parts, the bound state ψ_0 and the continuum part ψ_c, then the time-varying part of the dipole is [19]

$$\mathbf{d}(t) = \langle \psi_0(\mathbf{r}, t) | \mathbf{r} | \psi_c(\mathbf{r}, t) \rangle + \text{c.c.} \quad (3)$$

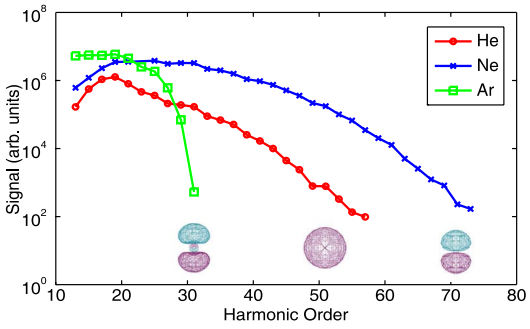

FIG. 1 (color online). High harmonic signals recorded for three atoms under identical experimental conditions. Also shown are the calculated orbital shapes for He ($1s$), Ne ($2p$), and Ar ($3p$).

We expand ψ_c as a sum of plane waves, which forms a complete basis set,

$$\psi_c(\mathbf{r}, t) = \int a(\omega) e^{i\mathbf{k}(\omega)\cdot\mathbf{r} - i\omega t} d\omega. \quad (4)$$

Here, $a(\omega)$ are the complex amplitudes of the plane wave components. Note that atomic units are used here, $\hbar = e = m_e = 1$; in atomic units, velocity, momentum, and wave number are the same, $v = p = k$. The function $k(\omega)$ and its inverse $\omega(k)$ relate the plane wave momentum k to its kinetic energy ω as $\omega(k) = k^2/2$.

Now the radiated signal in Eq. (1) can be written as

$$S(\Omega) = 4\pi^2 \Omega^4 |a(\omega) \langle \psi_0 | r | e^{ik(\omega)x} \rangle|^2. \quad (5)$$

Here, Ω is the emitted xuv frequency, and ω is the kinetic energy of the electron. These are related through $\Omega = \omega + I_p$ that comes from the delta function in the integral, and also comes from stationary phase points in SFA theory [8]. Later, we will discuss how to relate Ω and k.

Orbital wave functions were calculated using a standard Hartree-Fock *ab initio* program GAMESS [20], and the matrix elements from the highest orbitals to continuum plane waves of momentum k were calculated, $\langle \psi_0 | x | k \rangle$. For p orbitals, the orbital aligned with the laser field ($m = 0$) was chosen, since this will have the highest ionization rate [21]. The orbitals are shown in Fig. 1.

The calculated dipole matrix elements in the length gauge are shown in Fig. 2 for the three atoms. We show two slightly different calculations, depending on the choice of the function $\omega(k)$, as described in the caption.

The spectral amplitude $|a(\omega)|$ of the recollision electron wave packet can be determined from the experimental data in Fig. 1 by dividing by the matrix elements for each atom. The result is shown in Fig. 3. The wavelength dependence of the xuv grating [22] and of the MCP detector [23] has

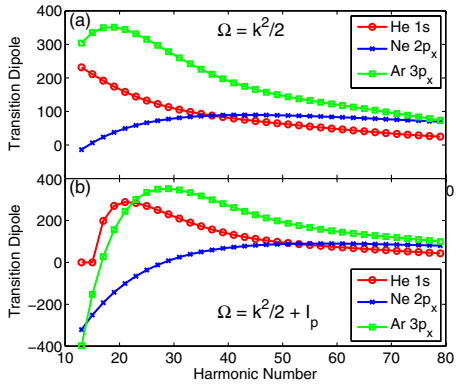

FIG. 2 (color online). Length gauge transition dipole matrix elements $\langle \psi_0 | x | k \rangle$ between each atom's HOMO, ψ_0, and a plane wave of momentum k, plotted against emitted xuv frequency Ω in multiples of the driving laser frequency. In (a), the field-free electron dispersion relation is used, $\Omega = k^2/2$. In (b), the ionization potential, I_p, has been subtracted from the emitted xuv frequency, Ω, to determine the corresponding plane wave momentum, k: $\Omega = k^2/2 + I_p$.

been removed from the measurements. The curves have been shifted vertically to compensate for differing overall efficiency and gas density.

The horizontal axis corresponds to the electron kinetic energy ω just *before* the electron encounters the ion's Coulomb potential. The lowest ("threshold") harmonics correspond to electrons returning with nearly zero kinetic energy where Coulomb effects become significant; we expect that the SFA model [8] breaks down here. It is evident that the results in Fig. 3 are largely independent of the atom, to within a vertical scaling factor due to differing overall ionization rates and gas densities. We hypothesize that the continuum wave packet is independent of the details of the atomic orbital from which it ionizes.

Why do we expect the plane wave amplitude $a(\omega)$ to be largely independent of the atomic orbital? The current theories of tunnel ionization (ADK [24], Yudin and Ivanov [25], molecular ADK [26]) are based on the instantaneous quasistatic tunneling rate written in the form

$$\Gamma_{\mathrm{qs}}(t) = A_{n,l}B_{l,|m|}I_p C(\theta)\left(\frac{2(2I_p)^{3/2}}{E_0}\right)^{2n-|m|-1} \times \exp\left(-\frac{2(2I_p)^{3/2}}{3E_0|\cos\omega t|}\right) \quad (6)$$

where E_0 is the peak electric field, n, l, m are the quantum numbers of the orbital, and t is time within the optical cycle. This expression contains an exponential part that depends on the phase within the optical cycle, and a preexponential part that contains details of the atomic or molecular orbital but not the phase. Since the quantum numbers do not appear in the exponential part that determines the cycle dependence of the ionization rate, we expect that the time dependence of the continuum wave packet does not depend on the orbital details. This is supported by the results shown in Fig. 3. The inferred continuum wave packet amplitudes are the same for all three atoms, to within the vertical scaling factor that comes from the atom-dependent preexponential factor. It is also supported by recent direct measurements of the electron velocity distribution for different alignments of the N_2 molecule [27].

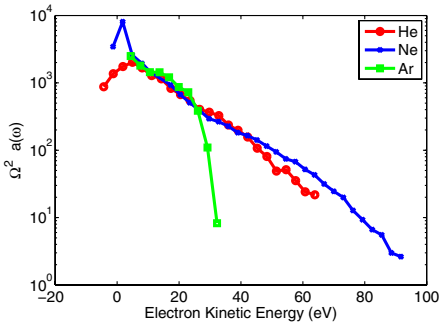

FIG. 3 (color online). The recorded HHG spectra were divided by the transition dipole in the length gauge for each atomic orbital to yield the amplitude of the continuum electron wave packet as it returns to the atom. We plot $\Omega^2|a(\omega)| = \sqrt{S(\Omega)}/|D_{\mathrm{len}}(k)|$ and utilize the dispersion relation $\Omega = k^2/2$. Because the laser intensity was well above the saturation intensity for argon, argon's higher harmonics fall off rapidly. The experimental data have been corrected for detector response and have been vertically scaled because of differing gas densities and ionization probabilities. The horizontal axis is the electron kinetic energy ω just before it interacts with the atomic potential, i.e., $\omega = \Omega - I_p$.

The calculation of transition dipole matrix elements depends on the gauge chosen [28]. The most common are length gauge ($D_{\mathrm{len}} = \langle\psi|r|k\rangle$), velocity gauge ($D_{\mathrm{vel}} = (i/\Omega)\langle\psi|v|k\rangle$), and acceleration gauge ($D_{\mathrm{acc}} = (1/\Omega^2)\times\langle\psi|\nabla V|k\rangle$, where V is the atomic potential). All three gauges should in principle yield the same result, but will differ if the wave functions are not eigenstates of the complete Hamiltonian of the system [28]. The acceleration gauge is commonly used in numerical calculations [18] where the model potential V is known, but in the present case, we have no *a priori* knowledge of the form of the potential which includes nonlocal effects due to the other electrons in the atoms. The use of a plane wave expansion could possibly result in a gauge dependence because the plane wave expansion employed by the strong field approximation (SFA) [8] ignores the Coulomb potential. Only recently have approximate solutions for the Coulomb-Volkov problem become available [29].

The treatment of the experimental spectra that was shown in Fig. 3 is repeated in Fig. 4 using both length and velocity gauges. Both gauges give good agreement up to a vertical scaling factor. This demonstrates that calculations done in both the length and velocity gauges agree, but require that the dispersion relation for the electron be slightly different. When the gauges and dispersion relations were reversed to that shown in Fig. 4, there was significant deviation from straight lines. We also tried

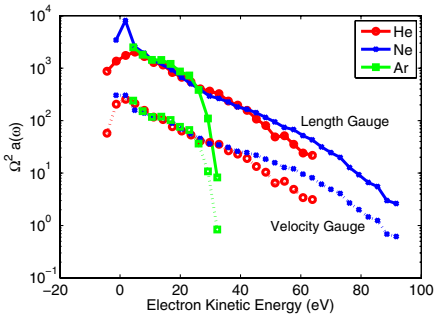

FIG. 4 (color online). Experimental high harmonic spectra from Fig. 1 divided by the transition dipole matrix elements calculated using both the length (solid lines) and the velocity gauge (dashed lines). In the lower group, we plot $\Omega^2|a(\omega)| = \sqrt{S(\Omega)}/|D_{\mathrm{vel}}(k)|$ and utilize the dispersion relation $\Omega = k^2/2 + I_p$. The length gauge curves are repeated from Fig. 3 to show that both gauges give similar results. The two gauges have been vertically displaced so that they can be compared.

using the acceleration gauge suggested by Gordon *et al.* [30], $D_{\mathrm{acc}} = (1/\Omega^2)\langle\psi|x/r^3|k\rangle$, but found that the agreement between atoms was poor for any choice of dispersion relation.

An uncertainty in the choice of the dispersion relation has been previously reported in the literature. Experiments with N_2 [11] use $\Omega = k^2/2$, whereas experiments with CO_2 indicate that $\Omega = k^2/2 + I_p$ is better [31]. Simulations for H_2^+/H_2 by Lein *et al.* [32] were found to be in qualitative agreement with a semiclassical model with $\Omega = k^2/2$, although the simulations gave results intermediate between $\Omega = k^2/2$ and $\Omega = k^2/2 + I_p$.

We have shown that we can use HHG to characterize the spectral amplitude $|a(\omega)|$ of the electron wave packet produced by tunnel ionization of atoms. The amplitude is largely independent of the shape of the atomic orbital that is ionized, as well as its ionization potential, for the three atoms tested, to the extent that HHG phase mismatch effects are not present. Both the length gauge and the velocity gauge give similar results, provided that we choose the correct dispersion relation. We hypothesize that this is a general behavior, but this must be further tested with other atoms and molecules. Our results suggest that it is easy to find a reference atom with which to calibrate $|a(\omega)|$ for molecular orbital tomography experiments [11]. It also confirms the functional form of the expression for the instantaneous tunnel ionization rate and sheds new light on the dispersion relation for the recombination electron and the gauge invariance of the transition dipoles. Further theoretical investigation of the relationship between gauge and dispersion relation is warranted.

We would like to thank Vladimir Yakovlev for performing the HHG propagation calculations for us.

*Electronic address: david.villeneuve@nrc.ca

[1] R. Rosman, G. Gibson, K. Boyer, H. Jara, T. S. Luk, I. A. McIntyre, A. McPherson, J. C. Solem, and C. K. Rhodes, J. Opt. Soc. Am. B **5**, 1237 (1988).
[2] A. L'Huillier and P. Balcou, Phys. Rev. Lett. **70**, 774 (1993).
[3] A. L'Huillier, D. Descamps, A. Johansson, J. Norin, J. Mauritsson, and C.-G. Wahlström, Eur. Phys. J. D **26**, 91 (2003).
[4] C. Lyngå, M. B. Gaarde, C. Delfin, M. Bellini, T. W. Hänsch, A. L Huillier, and C.-G. Wahlström, Phys. Rev. A **60**, 4823 (1999).
[5] M. Drescher, M. Hentschel, R. Kienberger, M. Uiberacker, V. Yakovlev, A. Scrinzi, T. Westerwalbesloh, U. Kleineberg, U. Heinzmann, and F. Krausz, Nature (London) **419**, 803 (2002).
[6] J. Seres, E. Seres, A. J. Verhoef, G. Tempea, C. Streli, P. Wobrauschek, V. Yakovlev, A. Scrinzi, C. Spielmann, and F. Krausz, Nature (London) **433**, 596 (2005).
[7] P. B. Corkum, Phys. Rev. Lett. **71**, 1994 (1993).
[8] M. Lewenstein, P. Balcou, M. Y. Ivanov, A. L'Huillier, and P. B. Corkum, Phys. Rev. A **49**, 2117 (1994).
[9] L. C. Dinu, H. G. Muller, S. Kazamias, G. Mullot, F. Augé, P. Balcou, P. M. Paul, M. Kovaĉev, P. Breger, and P. Agostini, Phys. Rev. Lett. **91**, 063901 (2003).
[10] Y. Mairesse, A. de Bohan, L. J. Frasinski, H. Merdji, L. C. Dinu, P. Monchicourt, P. Breger, M. Kovacev, R. Taeb, and B. Carré *et al.*, Science **302**, 1540 (2003).
[11] J. Itatani, J. Levesque, D. Zeidler, H. Niikura, H. Pépin, J. C. Kieffer, P. B. Corkum, and D. M. Villeneuve, Nature (London) **432**, 867 (2004).
[12] J. Itatani, D. Zeidler, J. Levesque, H. Niikura, D. M. Villeneuve, and P. B. Corkum, Phys. Rev. Lett. **94**, 123902 (2005).
[13] P. Balcou, R. Haroutunian, S. Sebban, G. Grillon, A. Rousse, G. Mullot, J. P. Chambaret, G. Rey, A. Antonetti, and D. Hulin *et al.*, Appl. Phys. B **74**, 509 (2002).
[14] A. Rundquist, C. D. Durfee, III, Z. Chang, C. Herne, S. Backus, M. M. Murnane, and H. C. Kapteyn, Science **280**, 1412 (1998).
[15] E. Constant, D. Garzella, P. Breger, E. Mével, C. Dorrer, C. Le Blanc, F. Salin, and P. Agostini, Phys. Rev. Lett. **82**, 1668 (1999).
[16] G. V. Marr and J. B. West, At. Data Nucl. Data Tables **18**, 497 (1976).
[17] V. Yakovlev (private communication).
[18] K. Burnett, V. C. Reed, J. Cooper, and P. L. Knight, Phys. Rev. A **45**, 3347 (1992).
[19] J. B. Watson, A. Sanpera, K. Burnett, and P. L. Knight, Phys. Rev. A **55**, 1224 (1997).
[20] M. W. Schmidt, K. K. Baldridge, J. A. Boatz, S. T. Elbert, M. S. Gordon, J. J. Jensen, S. Koseki, N. Matsunaga, K. A. Nguyen, and S. Su *et al.*, J. Comput. Chem. **14**, 1347 (1993).
[21] T. Otobe, K. Yabana, and J.-I. Iwata, Phys. Rev. A **69**, 053404 (2004).
[22] J. Edelstein, M. C. Hettrick, S. Mrowka, P. Jelinsky, and C. Martin, Appl. Opt. **23**, 3267 (1984).
[23] R. Hemphill, J. Edelstein, and D. Rogers, Appl. Opt. **36**, 1421 (1997).
[24] M. V. Ammosov, N. B. Delone, and V. P. Krainov, Sov. Phys. JETP **64**, 1191 (1986).
[25] G. Yudin and M. Y. Ivanov, Phys. Rev. A **64**, 013409 (2001).
[26] X. M. Tong, Z. X. Zhao, and C. D. Lin, Phys. Rev. A **66**, 033402 (2002).
[27] D. Zeidler, A. B. Bardon, A. Staudte, D. M. Villeneuve, R. Dörner, and P. B. Corkum, J. Phys. B **39**, L159 (2006).
[28] H. A. Bethe and E. E. Salpeter, *Quantum Mechanics of One- and Two-Electron Atoms* (Springer, Berlin, 1957).
[29] O. Smirnova, M. Spanner, and M. Y. Ivanov, J. Phys. B **39**, S307 (2006).
[30] A. Gordon, F. X. Kärtner, N. Rohringer, and R. Santra, Phys. Rev. Lett. **96**, 223902 (2006).
[31] C. Vozzi, F. Calegari, J.-P. Caumes, G. Sansone, S. Stagira, M. Nisoli, R. Torres, E. Heesel, N. Kajumba, and J. P. Marangos *et al.*, Phys. Rev. Lett. **95**, 153902 (2005).
[32] M. Lein, N. Hay, R. Velotta, J. P. Marangos, and P. L. Knight, Phys. Rev. A **66**, 023805 (2002).